

NACA TN 4055 888

0066726



NATIONAL ADVISORY COMMITTEE FOR AERONAUTICS

TECHNICAL NOTE 4055

EFFECTS OF AIRPLANE FLEXIBILITY ON WING BENDING

STRAINS IN ROUGH AIR

By Thomas L. Coleman, Harry Press,
and C. C. Shufflebarger

Langley Aeronautical Laboratory
Langley Field, Va.



Washington

July 1957

AFMDC
TECHNICAL LIBRARY
AFL 2811



TECHNICAL NOTE 4055

EFFECTS OF AIRPLANE FLEXIBILITY ON WING BENDING

STRAINS IN ROUGH AIR

By Thomas L. Coleman, Harry Press,
and C. C. Shufflebarger

SUMMARY

Some results on the effects of wing flexibility on wing bending strains as determined from flight tests of a Boeing B-29 and a Boeing B-47A airplane in rough air are presented, and the experimental results for the B-29 airplane are compared with results from an analytical study. The results are presented as frequency-response functions of the bending strains at various spanwise wing stations to gust disturbances. For the B-29 airplane, the effects of the first and second symmetrical bending modes yield moderate strain amplifications in rough air all along the airplane span. Calculations involving one or preferably two structural modes appear to yield reliable estimates of the flexibility effects on the strains. For the B-47A airplane, the dynamic amplifications appear to be quite large, particularly in the midspan region, but these amplifications are partially balanced by large and favorable static aeroelastic effects associated with this swept-wing airplane. In addition, some indirect results from the B-47A investigation suggest that spanwise variations in turbulence have a significant effect on the responses of airplanes with large spans.

INTRODUCTION

Previous flight investigations (refs. 1 to 3) have indicated that wing flexibility could cause substantial amplification in the wing strains in rough air for such straight-wing airplanes as the Douglas DC-3, Martin 2-0-2, and the Boeing B-29. Also, by application of power-spectral methods of analysis, good correlation has been obtained between the measured root bending strains and calculated results for these three airplanes (ref. 3). As a continuation of the work in this area, the B-29 investigation has been extended to cover the bending-strain amplifications at several other wing stations. In addition, a flight investigation involving the swept-wing Boeing B-47A airplane has been undertaken in order to assess the significance of the wing sweep on the elastic response in rough air.

In the present paper, an effort is made to summarize some of the more important results obtained in recent extensions of the studies involving the B-29 and B-47A airplanes. The material to be covered includes experimental results on the bending-strain responses at various stations for both the Boeing B-29 and the Boeing B-47A airplanes. For the B-29 airplane investigation, comparisons are made between the experimental results and calculations. Unfortunately, similar results are not yet available for the B-47A investigation. The present paper is concerned with describing the response characteristics of these airplanes in terms of their strain frequency-response functions to atmospheric turbulence. Finally, some indirect evidence obtained in the B-47A investigation on the effects of spanwise variations in turbulence on the strain and acceleration responses is described.

AIRPLANES, INSTRUMENTATION, AND TEST CONDITIONS

Figure 1 shows plan-form views of the two test airplanes and the locations of some of the primary instrumentation. The basic instrumentation of the two airplanes included strain gages (denoted by the small + signs) to measure bending- and shear-strain indications on the front and rear spars at 5 spanwise stations. Accelerometers were installed at a number of locations on the airplanes. The accelerometer measurements pertinent to the present paper are shown by the shaded circles on the figures and were at the nodal points of the fundamental wing bending mode of the B-29 airplane and at the center of gravity of the B-47A airplane. In addition to the accelerometers and strain gages, the instrumentation included control position recorders and attitude and rate gyros. One significant addition to the B-47A instrumentation was a flow-direction vane from which a time history of the vertical gust velocity could be derived by correcting the vane measurements for airplane motions.

Relative to the present investigations, these two airplanes differed in a number of respects. The airplane weights were about the same with the test weight of the B-29 airplane at 105,900 pounds and the weight of the B-47A airplane at 113,200 pounds. However, the B-29 airplane had a far greater proportion of its total weight (about 80 percent) in the wings since almost all the fuel was in wing tanks. The B-47A carries all its fuel in the fuselage, and the ratio of the wing weight to total weight for this airplane was 36 percent. In addition to the differences in the proportion of weight in the wing, the wing weight of the B-29 was relatively uniformly distributed over the span, whereas the distribution of wing weight for the B-47A was typified by large concentrated masses due to engine nacelles. The airplanes also differed significantly in stiffness with the wing of the B-29 airplane being about twice as stiff as that of the B-47A airplane. A further difference, which will be of some

consequence in the results to be presented, arises from the swept wing of the B-47A. Because of the swept wing, the lower stiffness, and the concentrated masses, the B-47A airplane has rather large static aeroelastic effects associated with wing twist; in contrast, such aeroelastic effects are negligible or absent on the B-29 airplane and on the other airplanes studied.

The flight tests for both airplanes were in clear air turbulence at an altitude of about 2,000 feet above terrain. The flight test speeds were 250 miles per hour for the B-29 airplane and 478 miles per hour for the B-47A airplane. The basic test results were obtained in flight test runs of several minutes duration in continuous rough air for each of these test airplanes. In addition to the rough-air tests, slow maneuver pull-ups were also made in smooth air at various test conditions in order to determine quasi-static reference strains.

METHODS FOR DETERMINATION OF FREQUENCY RESPONSE

In discussing the results of these investigations, the basic quantity that will be used is the frequency-response functions of the wing strains or accelerations to gust disturbances. This function describes the airplane response in strain or in normal acceleration, as the case may be, to unit sinusoidal gusts of various frequencies. The airplane response to continuous rough air depends essentially on the product of the amplitude squared of the frequency-response function and the power spectrum of the gust velocity. Two basic approaches may be used for the experimental determination of the frequency-response functions to gust inputs, and these are given as follows: The first method, called the spectrum method, is based upon the relation between the power spectrum of a random disturbance and the power spectrum of the response of a linear system to the disturbance. From this relation, the amplitude squared of the frequency-response function is given by

$$|H(f)|^2 = \frac{\Phi_o(f)}{\Phi_1(f)}$$

where

$ H(f) ^2$	amplitude squared of frequency-response function
$\Phi_o(f)$	power spectrum of airplane response
$\Phi_1(f)$	power spectrum of disturbance or gust input

The application of this method simply requires the measurement of the response power spectrum Φ_0 and the power spectrum of the gust input Φ_1 .

The second method designated as the cross-spectrum method is based upon the relationship for linear systems between a random input disturbance and the cross spectrum between the input disturbance and the system response to the disturbance (ref. 4). From this relationship, the frequency-response function is given by the following expression:

$$H(f) = \frac{\Phi_{10}(f)}{\Phi_1(f)}$$

where $\Phi_{10}(f)$ is the cross spectrum between the disturbance input and the airplane response. In this second method both the amplitude and phase of the frequency-response function $H(f)$ are obtained since $\Phi_{10}(f)$ is, in general, complex.

In the material to be presented, both of these methods will be applied. It should be noted that if the measurements of turbulence such as that obtained from the angle-of-attack vane adequately represent the gust input, then the two methods should yield identical results for the amplitude of the frequency-response function. If, however, complicating factors are present, such as significant variations in turbulence across the airplane span, the results obtained by the two methods will differ (see appendix). In the following material, this property will be used in assessing the significance of spanwise variations in the turbulence on the test results.

RESULTS FOR THE B-29 AIRPLANE

The measurements obtained in the course of the B-29 flight investigation have been used to estimate the frequency-response function for the bending strains at the various stations by application of the spectrum method described in the preceding section. In estimating the frequency-response function, it was necessary to assume a shape for the gust spectrum since the gust spectrum was not measured in the B-29 investigation. The gust spectrum used for this purpose is given by the following expression:

$$\Phi(\Omega) = \sigma^2 \frac{L}{\pi} \frac{1 + 3\Omega^2 L^2}{(1 + \Omega^2 L^2)^2}$$

where $\Omega = 2\pi f/V$ and V is the airplane speed. This spectrum has been found to approximate the atmospheric conditions covered by flight measurements of gust spectra when a value of about 1,000 is used for the scale of the turbulence L . The intensity of the turbulence which is described by the root-mean-square gust velocity σ is, however, not known for the B-29 measurements.

In order to permit direct comparisons of the frequency-response functions at the various wing stations, the results were converted to "equivalent accelerations" by dividing the strains at each station by the strain per g measured at the station during slow pull-ups. The results obtained for the amplitude of the frequency-response function on this basis are shown in figure 2. The ordinate represents the amplitude of the bending-strain response for a unit sinusoidal gust velocity at the various frequencies. The four solid-line curves shown in the figure are the results for the four spanwise stations whose locations are designated in terms of the fraction of the semispan $\frac{y}{b/2}$. Also shown in figure 2, by the dashed-line curve, is the frequency-response function obtained from the measured nodal accelerations. This frequency-response function can be considered as a reference for static loading. Thus, the difference between this reference and the other curves gives an indication of the effects of wing flexibility. (Flexibility also has an effect on the nodal accelerations, but this effect is small for this airplane.)

Comparison of the solid curves of figure 2 with the reference curve of nodal acceleration shows that the principal effects of flexibility are associated with a large peak at the first bending mode, which is at 2.7 cps. The amplification is highest for the 15-percent-semispan station and progressively decreases with outboard wing span station.

In order to see how well the frequency-response functions for the B-29 airplane could be determined analytically, calculations were also made. The calculated strain frequency-response functions were converted to equivalent accelerations for direct comparison with the results of figure 2 and are shown in figure 3. These results are for three modes or degrees of freedom, that is, airplane vertical motion and the first and second symmetrical bending modes. Comparison of the results in figures 2 and 3 shows that, in general, the character and trends of the experimental and calculated frequency-response functions are in fairly good agreement in regard to flexibility effects. Both figures indicate that the principal effects of flexibility are associated with the first bending mode and that the amplification is largest at the root station and progressively decreases with outboard wing span station.

It is of interest to note that the calculated and measured frequency-response functions (figs. 2 and 3) differ below about 1 cps. This difference is due principally to the omission of the pitching motion in the

calculations. Because of the high gust input power at these low frequencies, it would thus appear that the inclusion of the pitching mode is quite important in determining the actual output response.

The effect which the frequency-response functions have on the overall bending-strain amplification is shown in figure 4. In the upper part of the figure, the ordinate is the ratio of the root-mean-square strain for the flexible airplane $\sigma_{\epsilon, \text{FLEX}}$ to the root-mean-square strain for the reference condition $\sigma_{\epsilon, \text{REF}}$. The reference strains were based on the nodal-point accelerations measured in rough air and the strain per g as measured at the various spanwise stations in slow pull-ups. This reference condition represents the strains for the static application of loads, and thus this ratio provides a measure of dynamic-strain amplification. The circles represent the measured amplification factors, and the curves represent calculated results. The dashed curve was obtained by considering two modes: airplane vertical motion and the first symmetrical mode in bending. The solid curve was obtained by using three modes: airplane vertical motion and the first two symmetrical bending modes. The measured results show that the overall strain amplification is approximately 10 percent at the root station and is somewhat lower at the outboard wing stations. Both the two-mode and three-mode calculations are in rather good agreement with the measured results except at the farthest outboard station.

A second set of strain-amplification factors is shown in the lower part of figure 4. This ordinate is the ratio of the peak strains that would occur with equal frequency for the flexible airplane ϵ_{FLEX} and for the reference airplane condition ϵ_{REF} . The frequency level at which this strain ratio was taken corresponds to a value of strain equal to about twice the root-mean-square strain. These experimental amplifications are about twice as large as those shown in the top figure based on root-mean-square strains. This is a consequence of flexibility having a greater effect on the number of peak strains than on the root-mean-square values. The calculations which use only two modes underestimate the strain amplifications at the outboard stations, whereas the analysis using three modes gives a good approximation to the measured results.

The foregoing results imply that, for this straight-wing airplane, calculations using only vertical motion and the fundamental bending mode are adequate for determining the effects of flexibility on the root-mean-square strain values but that the second bending mode must also be included when considering peak strains.

RESULTS FOR THE B-47A AIRPLANE

Frequency-Response Functions

The rest of this paper will cover test results obtained from the B-47A airplane investigations. Figure 5 shows the measured frequency-response functions for the rear-spar bending strains for various wing stations. Similar results were also obtained for the strains on the front spar but are not included. The results shown are for both the amplitude and the phases and were obtained by the cross-spectrum method. The gust input spectrum was obtained from the vane angle-of-attack measurements corrected for airplane motions according to the method given in reference 5. For present comparisons, the measured strains at the various stations were converted to equivalent accelerations by dividing by the strains per g in pull-ups at the same test conditions. The reference curve shown in the figure was based on the center-of-gravity accelerations which appear to be relatively uninfluenced by the fundamental airplane vibration mode and provides a measure of the strains for static loading. (The use of the center-of-gravity accelerations for the reference loading is discussed in more detail later.) The differences between the reference curve and the other curves thus provide a direct measure of the effects of the dynamic flexibility on the local strains. As in the case of the B-29, the effects of flexibility show up principally as a large peak at the first bending mode frequency which is around $1\frac{1}{2}$ cps. In contrast to the B-29, however, the magnitude of the peak is now smallest at the root station and progressively increases for the outboard stations. Another significant difference between the frequency-response functions for the B-47A and the B-29 airplanes is the closer proximity of the first bending mode to the short-period mode which is at about 0.6 cps. As a consequence, the gust input, which decreases rapidly with frequency, will be relatively much higher at the first bending mode in this case, and larger overall amplification effects may be expected.

The phases shown in figure 5(b) indicate a linear increase in phase lag with increasing frequency, as is the case for a simple system with a moderate amount of damping. Above 2 cps, the curves appear to be erratic. The results above 2 cps are not, however, considered to be reliable.

Strain-Amplification Factors

Figure 6 shows the variations in the bending-strain-amplification factors with spanwise positions. Again, the results are shown based on both root-mean-square values and strains having an equal frequency of occurrence. Note that the ordinate scale is compressed and covers a wider range of amplification values than the scale used earlier for the corresponding B-29 results.

For the swept-wing airplane, the effects of flexibility are complicated by large static aeroelastic or twist effects which act to reduce the gust loading and the strain response. Thus, the derivation of amplification factors for this case is not straightforward, and several procedures might be used. For present purposes, three strain responses are considered. These are the actual measured strains, the numerator of the ordinate, and two reference strain conditions. These reference strains are

- (1) The strains obtained by the static application of the same loads to the airplane.
- (2) The strains obtained by the static application of the loads to an essentially "rigid" airplane, that is, an airplane embodying no static aeroelastic effects.

The ratio of the measured strains to the strains in the statically elastic airplane yields the solid-line curves and provides a measure of the purely dynamic strain amplification. (See fig. 6.) The ratio of the measured strains to the strains for the airplane without static aeroelastic effects yields the dashed-line curves and provides a measure of the combined effects of the static alleviation and the dynamic amplification.

The procedure used in the determination of the reference strains was based upon the use of the actual measured center-of-gravity accelerations as a measure of the airplane loading in rough air. Examination of the power spectra of the normal accelerations had indicated that the first mode had only a minor effect on the center-of-gravity accelerations. As a further check, the average airplane acceleration was determined for a short section of the test run by using the accelerometer measurements from 22 locations along the wing and fuselage of the test airplane along with their associated masses. The results obtained indicated that, except for the presence of high-frequency fluctuations associated with the higher structural modes, the center-of-gravity acceleration provided a good measure of the airplane acceleration. On this basis, the center-of-gravity acceleration measurements were faired to remove the effects of the higher structural modes and used as a measure of the airplane loading. The loads obtained on this basis were then converted to strains for the various stations on a static basis by using the strains per g as measured in slow pull-up maneuvers at the test dynamic pressure. The strains obtained on this basis provide a measure of the strains for a statically elastic airplane and were used in obtaining the solid-line curves of figure 6.

In order to provide a measure of the static-aeroelastic effects on the strains, the strains per g in pull-ups were also determined for the condition of low or zero dynamic pressure. At low dynamic pressure, the static aeroelastic effects tend to be minimized, and thus the strains per g obtained at low dynamic pressure provide a basic "rigid" airplane reference condition. Figure 7 illustrates the values of bending strain

per g obtained at one station ($\frac{y}{b/2} = 0.60$) for various values of dynamic pressure. The variation of the strain per g appears linear over the wide range of dynamic pressure represented. A linear extrapolation to a value of dynamic pressure of 0 was therefore used. The difference between the strain per g (0.65) for a dynamic pressure of 0 and the value (0.51) for the test dynamic pressure provides a measure of the static aeroelastic strain alleviation for this station. The amount of this alleviation is about 22 percent for this station and varied somewhat for the other stations.

The strains per g for the condition at a dynamic pressure of 0 were used with the airplane center-of-gravity acceleration to obtain the second set of reference strains. These reference strains constitute strains for an airplane embodying no dynamic flexibility or static aeroelastic effects and were used to obtain the dashed curves of figure 6.

In the upper part of figure 6, the dynamic amplification, shown by the solid curve, is about 10 percent at the root but increases rapidly along the span and reaches a value of about 2 at the 60-percent-semispan station. The amplification factors obtained by considering both the static alleviation and dynamic effects, shown by the dashed line, are below 1 at the inboard stations but reach values of about 1.5 at the 60-percent-semispan station.

The amplification factors based on the ratios of strains for equal frequency of occurrence, shown in the lower part of figure 6, follow the same pattern as those based on the root-mean-square values but are everywhere higher. It thus appears that, for the swept-wing B-47A airplane, the effects of dynamic flexibility are quite large, particularly at the mid-span stations, but that favorable static aeroelastic alleviation moderates the large dynamic amplifications. In addition, it is evident that several values for the amplification factor may be obtained depending upon the particular definition or reference used. The particular amplification factor of significance depends upon the specific application.

EFFECTS OF SPANWISE VARIATIONS IN TURBULENCE

As a final point, some indirect evidence of the effects of spanwise variations in turbulence on airplane gust response will be presented. As mentioned previously, two methods could be used in determining the frequency-response functions for the B-47A: the spectrum and the cross-spectrum methods. As indicated, if no spanwise variations in turbulence existed, then the gust input would be adequately reflected by the point measurements of the angle-of-attack vane. For this case, both methods

should yield identical results for the frequency-response function. Figure 8 shows the frequency-response functions obtained by the two methods for the airplane center-of-gravity normal acceleration. It is quite clear that the cross-spectrum results are consistently lower than those obtained by the spectrum method. Similar differences also have been found between strain frequency-response functions obtained by the two methods. The differences between these two results are suggestive of the effects of spanwise variations in gusts which have received considerable attention recently in analytical studies by Diederich, Drischler, and Liepmann. (See refs. 6, 7, and 8.)

By making use of some results obtained by Diederich (ref. 6), first-order adjustments for the effects of spanwise variations of turbulence for the condition of isotropic turbulence were made to these two results in accordance with the analysis given in the appendix. The adjusted frequency-response functions obtained are shown in figure 9. Two effects may be noticed from this adjustment. First, the two frequency-response functions are now in much better agreement, and second, the adjustment has raised the two curves by from 10 to 20 percent over most of the frequency range in accordance with the span averaging functions of figure 10. The basis for the underestimation and distortion in the apparent frequency-response function of figure 8 stems from the fact that the point gust input used is too high. The effective gust input is the average gust velocity across the span which, as indicated in reference 6, tends to fall below the point input at all frequencies. As a consequence, the airplane acceleration response is lower than what would be expected for uniform distribution of the measured gust input across the span. These results thus suggest that the effects of spanwise variations in turbulence are significant for such airplanes as the B-47A. In addition, since analytic results indicate that the effects of spanwise variations in turbulence are primarily a function of span, these effects may be even more important for airplanes with larger span than the present airplane.

CONCLUDING REMARKS

It has been indicated that, for the B-29 airplane, the effects of the first and second symmetrical bending modes yield moderate strain amplifications in rough air all along the airplane span. Calculations involving one or preferably two structural modes appear to yield reliable estimates of flexibility on the strains.

For swept-wing airplanes, the effects of flexibility are complicated by the importance of static aeroelasticity effects in addition to the dynamic response. In the case of the B-47A airplane, the dynamic amplifications appear to be quite large, particularly in the midspan region.

These amplifications are at least partially balanced by large and favorable static aeroelastic effects associated with sweep. Finally, some indirect results suggest that spanwise variations in turbulence have a significant effect on the responses of the B-47A airplane.

Langley Aeronautical Laboratory,
National Advisory Committee for Aeronautics,
Langley Field, Va., March 5, 1957.

APPENDIX

EFFECTS OF SPANWISE VARIATIONS IN TURBULENCE ON
MEASURED FREQUENCY-RESPONSE FUNCTIONS

In the main body of this paper, it was indicated that, for uniform turbulence across the airplane span, the amplitude of the frequency-response function for gust disturbances $|H(f)|$ can be obtained experimentally by two methods; the spectral method which is based on the relation

$$|H_s(f)|^2 = \frac{\Phi_o(f)}{\Phi_1(f)} \quad (A1)$$

and the cross-spectral method which is based on the relation

$$H_c(f) = \frac{\Phi_{1o}(f)}{\Phi_1(f)} \quad (A2)$$

The subscripts s and c are used to differentiate between the estimates obtained by the two methods. In this appendix, the effects on these estimates of spanwise variations of turbulence will be outlined. The material to be presented is based on the analysis of the effects of spanwise gust variations given in reference 6.

The response of an airplane $z(t)$ to two-dimensional turbulence, that is, turbulence varying along the flight path and along the spanwise direction, may be expressed as

$$z(t) = \int_{-b/2}^{b/2} \int_{-\infty}^{\infty} x(t - t_1, y) h(t_1, y) dt_1 dy \quad (A3)$$

where

- b wing span
- $x(t, y)$ vertical gust velocity impinging at wing leading edge at time t and span location y
- $h(t, y)$ response at time t due to unit impulse gust impinging at wing between station y and $y + dy$ at time zero

The power spectrum of $z(t)$ as derived in reference 6 for the case of isotropic turbulence is given by

$$\Phi_z(f) = \int_{-b/2}^{b/2} \int_{-b/2}^{b/2} \Phi_x(f, y_2 - y_1) H(f, y_1) H^*(f, y_2) dy_1 dy_2 \quad (A4)$$

where

$\Phi_z(f)$ power spectrum of response $z(t)$

$\Phi_x(f, y_2 - y_1)$ cross-spectrum between gust velocities impinging at wing leading edge at stations y_2 and y_1

$H(f, y)$ influence function describing response of airplane to unit sinusoidal gusts impinging at wing leading edge at station y and is given by

$$H(f, y) = \int_0^{\infty} h(t, y) e^{-ift} dt$$

The asterisk designates the complex conjugate.

In these terms, the frequency-response function obtained by the spectral method can be expressed as

$$|H_S(f)|^2 = \frac{\int_{-b/2}^{b/2} \int_{-b/2}^{b/2} \Phi_x(f, y_2 - y_1) H(f, y_1) H^*(f, y_2) dy_1 dy_2}{\Phi(f, 0)} \quad (A5)$$

where $\Phi(f, 0)$ is the power spectrum of the gust input at span station 0 (such as measured with the vane).

The expression for $|H_S(f)|^2$ given by equation (A5) may be viewed as an average frequency-response function. Further insight into this result can be obtained by considering the special case

$$H(f, y) = H(f) \gamma(y) \quad (A6)$$

where

$$\int_{-b/2}^{b/2} \gamma(y) dy = 1$$

For this case

$$\begin{aligned}
 |H_S(f)|^2 &= |H(f)|^2 \left[\frac{\int_{-b/2}^{b/2} \int_{-b/2}^{b/2} \phi_x(f, y_2 - y_1) \gamma(y_1) \gamma(y_2) dy_1 dy_2}{\phi(f, 0)} \right] \\
 &= |H(f)|^2 \bar{\gamma}_1^2(f)
 \end{aligned}
 \tag{A7}$$

Equation (A7) indicates that the quantity $|H_S(f)|^2$ determined from measurements represents the "frequency part" of the frequency-response function multiplied by the term in brackets, which might be considered a span averaging function. For the case of uniform turbulence across the span, equation (A7) reduces to

$$|H_S(f)|^2 = |H(f)|^2$$

If the turbulence is isotropic with a known spectrum, the averaging function given by the term in brackets in equation (A7) can be evaluated. Evaluations of the numerator of the term in brackets are given in references 6 and 7 for several assumed power spectra of turbulence and for several assumed span distributions $\gamma(y)$. By using these results, the function $\bar{\gamma}_1(f)$ was evaluated for a particular case and the results obtained are shown in figure 10. The result shown in figure 10 is for the case of a uniform span distribution ($\gamma(y) = 1/b$) and a spectrum of vertical gust velocity given by

$$\phi(\Omega) = \sigma_w^2 \frac{L}{\pi} \frac{1 + 3\Omega^2 L^2}{(1 + \Omega^2 L^2)^2} \tag{A8}$$

where $\Omega = \frac{2\pi f}{V}$ and V is the airplane forward speed. In equation (A8), σ_w is the root-mean-square gust velocity and L is the scale of turbulence. A value of $L = 1,000$ feet appears to be representative of conditions for atmospheric turbulence. For present purposes, a value of $b/L = 0.1$ was assumed. The results of reference 7 indicate that the averaging function $\bar{\gamma}_1(y)$ is not sensitive to variation in $\gamma(y)$, sweep angle, and the form of the assumed gust spectrum.

A similar analysis may be applied to the cross-spectrum case and yields the following results:

$$H_c(f) = H(f) \left[\frac{\int_{-b/2}^{b/2} \Phi_x(f,y) \gamma(y) dy}{\Phi(f,0)} \right]$$

$$= H(f) \bar{\gamma}_2(f) \quad (A9)$$

where $\Phi_x(f,y)$ is the cross spectrum between the vertical gust velocities at span stations 0 and y . The weighting function given by the term in brackets may also be viewed as an average span weighting function $\bar{\gamma}_2(f)$. The function $\bar{\gamma}_2(f)$ can also be evaluated from figure 4 of reference 6 for the case of uniform span loading and the gust spectrum of equation (A8). This function $\bar{\gamma}_2(f)$ is also shown in figure 10.

If the weighting functions $\bar{\gamma}_1(f)$ and $\bar{\gamma}_2(f)$ given in equations (A7) and (A9) are divided into the measured values of $|H_B(f)|$ and $|H_C(f)|$, respectively, of figure 8, estimates of $|H(f)|$ may be obtained which are compatible. The results obtained in this manner are shown in figure 9.

REFERENCES

1. Mickleboro, Harry C., and Shufflebarger, C. C.: Flight Investigation of the Effects of Transient Wing Response on Wing Strains of a Twin-Engine Transport Airplane in Rough Air. NACA TN 2424, 1951.
2. Murrow, Harold N., and Payne, Chester B.: Flight Investigation of the Effect of Transient Wing Response on Wing Strains of a Four-Engine Bomber Airplane in Rough Air. NACA TN 2951, 1953.
3. Houbolt, John C., and Kordes, Eldon E.: Structural Response to Discrete and Continuous Gusts of an Airplane Having Wing-Bending Flexibility and a Correlation of Calculated and Flight Results. NACA Rep. 1181, 1954. (Supersedes NACA TN 3006; also contains essential material from TN 2763 and TN 2897.)
4. Press, Harry, and Tukey, John W.: Power Spectral Methods of Analysis and Their Application to Problems in Airplane Dynamics. Instrumentation Systems. Vol. IV of AGARD Flight Test Manual, Pt. IV C, Enoch J. Durbin, ed., North Atlantic Treaty Organization, pp. IVC:1-IVC:41.
5. Crane, Harold L., and Chilton, Robert G.: Measurements of Atmospheric Turbulence Over a Wide Range of Wavelength for One Meteorological Condition. NACA TN 3702, 1956.
6. Diederich, Franklin W.: The Response of an Airplane to Random Atmospheric Turbulence. NACA TN 3910, 1957.
7. Diederich, Franklin W., and Drischler, Joseph A.: Effect of Spanwise Variations in Gust Intensity on the Lift Due to Atmospheric Turbulence. NACA TN 3920, 1957.
8. Liepmann, H. W.: Extension of the Statistical Approach to Buffeting and Gust Response of Wings of Finite Span. Jour. Aero. Sci., vol. 22, no. 3, Mar. 1955, pp. 197-200.

TEST AIRPLANES

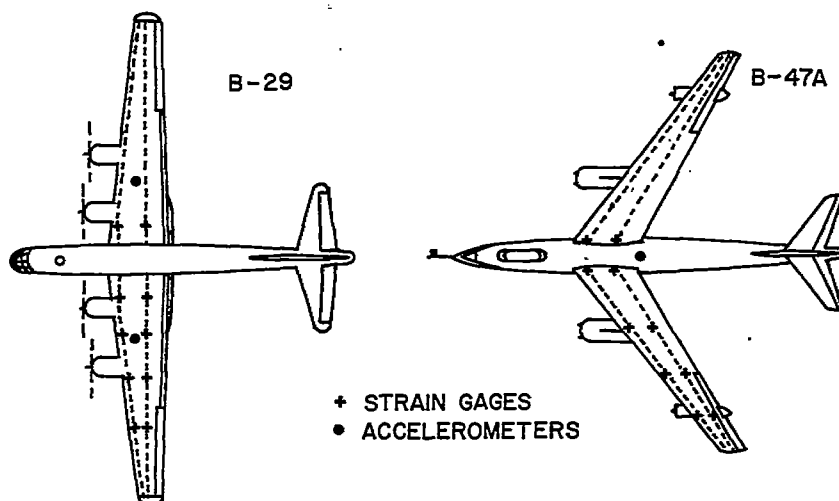


Figure 1

MEASURED B-29 STRAIN
FREQUENCY RESPONSE FUNCTION

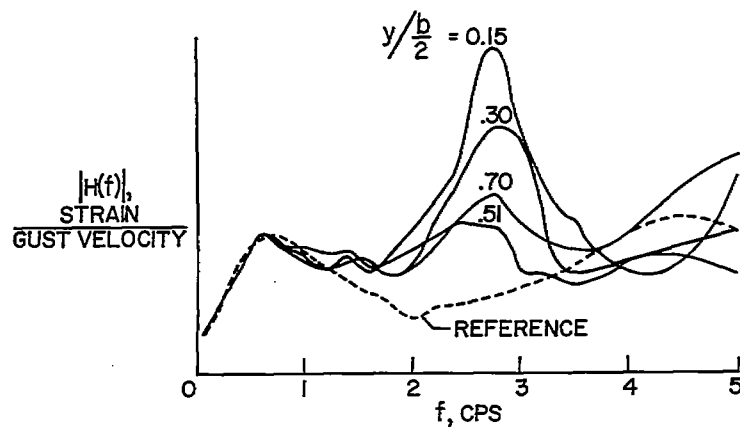


Figure 2

CALCULATED B-29 STRAIN
FREQUENCY RESPONSE FUNCTION

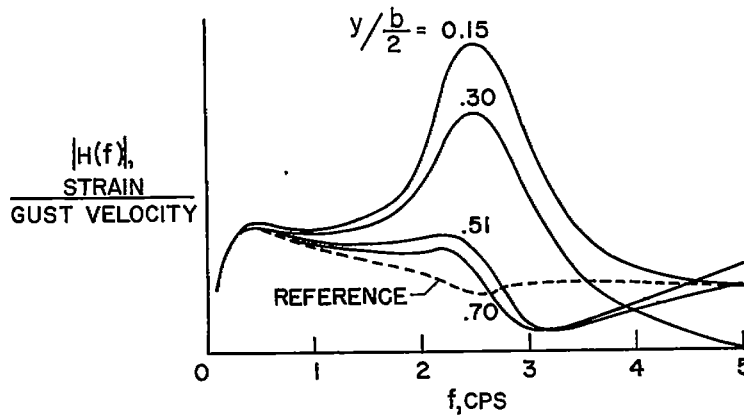


Figure 3

B-29 STRAIN AMPLIFICATION

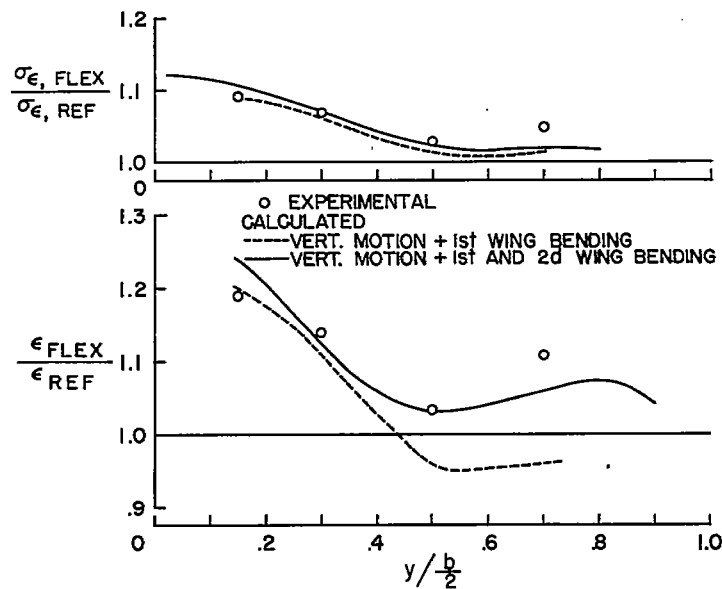


Figure 4

MEASURED B-47A STRAIN FREQUENCY-
RESPONSE FUNCTION
AMPLITUDE

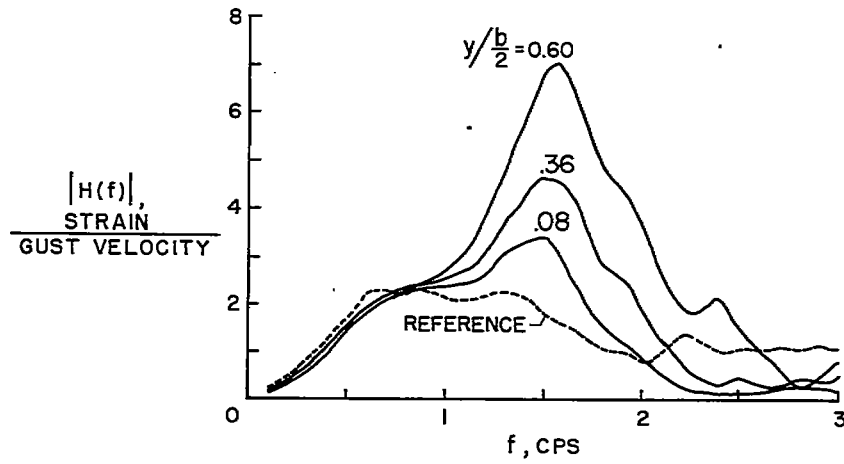


Figure 5(a)

MEASURED B-47A STRAIN FREQUENCY-RESPONSE FUNCTION
PHASE ANGLE

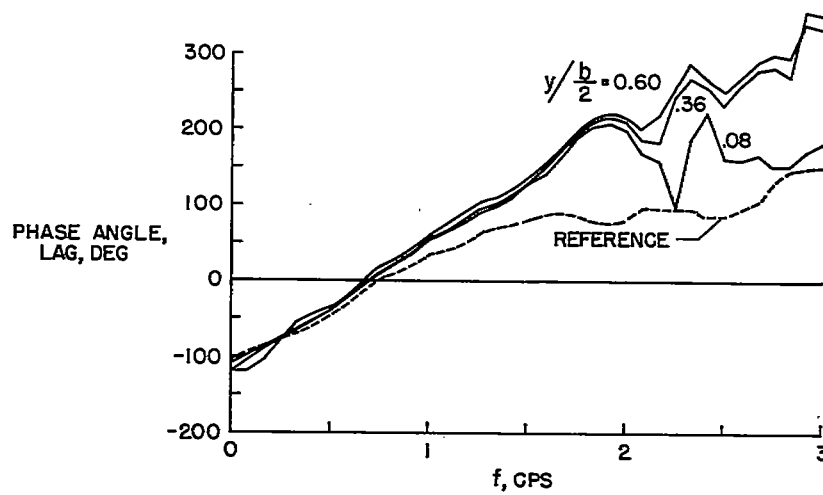


Figure 5(b)

B-47A STRAIN AMPLIFICATION

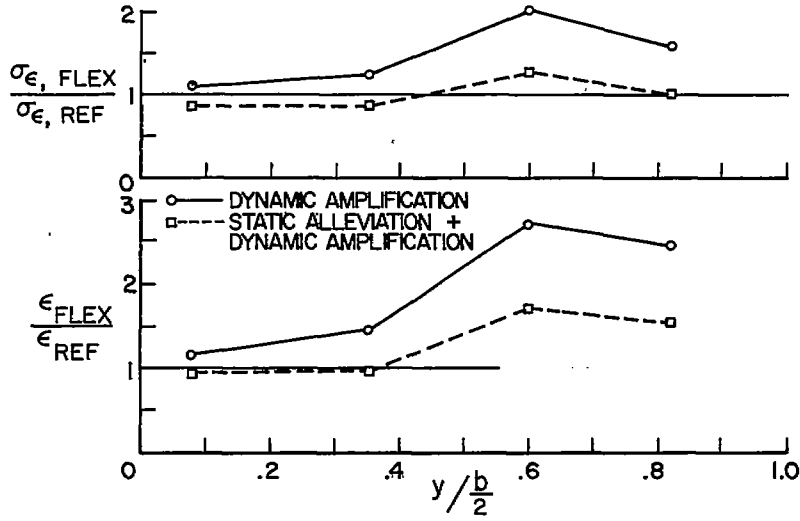


Figure 6

VARIATION OF STRAIN PER g IN PULL-UP WITH DYNAMIC PRESSURE

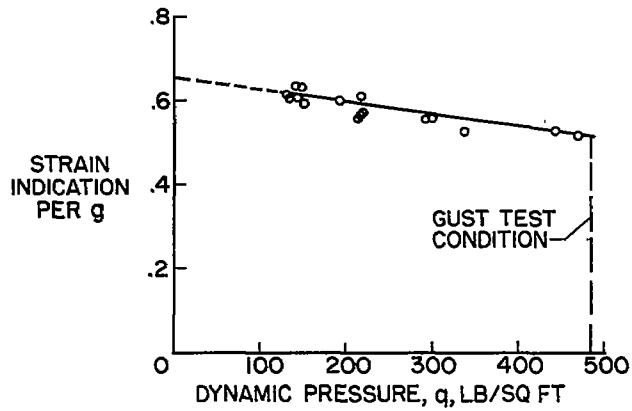


Figure 7

B-47A NORMAL—ACCELERATION FREQUENCY-
RESPONSE FUNCTION

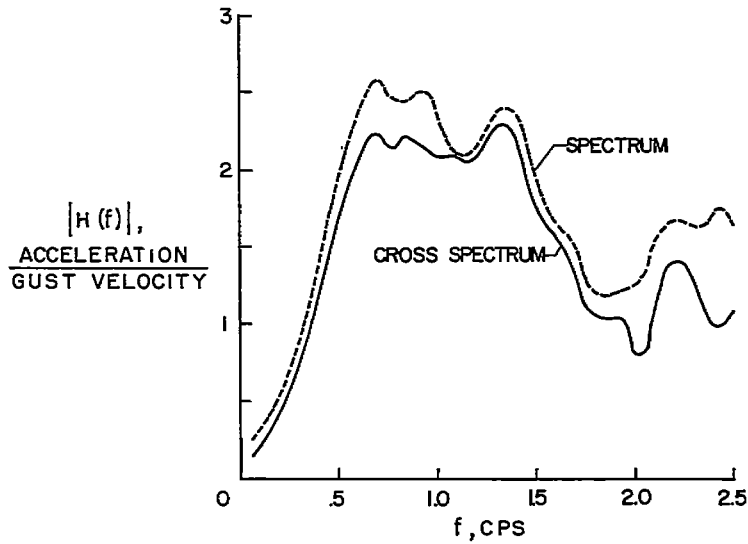


Figure 8

B-47A NORMAL—ACCELERATION FREQUENCY-
RESPONSE FUNCTION
ADJUSTED FOR SPANWISE GUST VARIATIONS

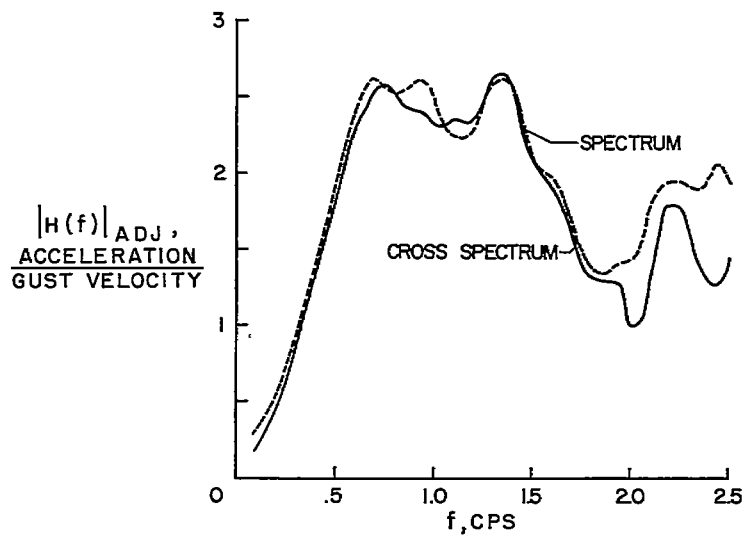


Figure 9

SPAN AVERAGING FUNCTIONS $\bar{\gamma}_1(f)$ AND $\bar{\gamma}_2(f)$ FOR $b/L=0.1$

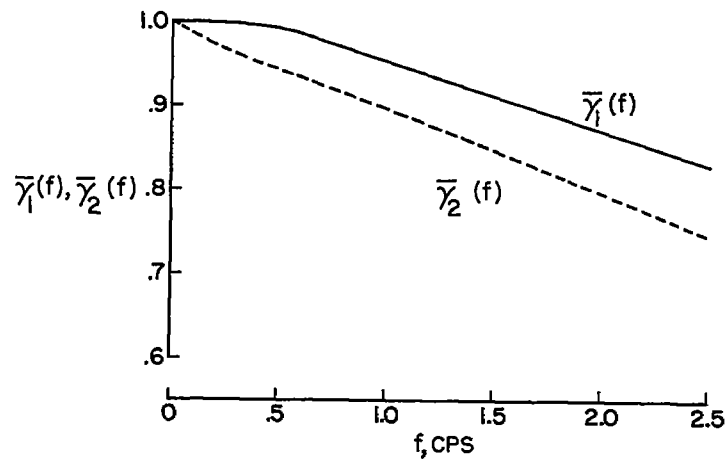


Figure 10